IceBridge PARIS L2 Ice Thickness, Version 1

USER GUIDE

How to Cite These Data

As a condition of using these data, you must include a citation:

Raney, K. 2010. *IceBridge PARIS L2 Ice Thickness, Version 1*. [Indicate subset used]. Boulder, Colorado USA. NASA National Snow and Ice Data Center Distributed Active Archive Center. https://doi.org/10.5067/OMEAKG6GIJNB. [Date Accessed].

FOR QUESTIONS ABOUT THESE DATA, CONTACT NSIDC@NSIDC.ORG

FOR CURRENT INFORMATION, VISIT https://nsidc.org/data/IRPAR2

National Snow and Ice Data Center

TABLE OF CONTENTS

1 DETAILED DATA DESCRIPTION

1.1 Format

The PARIS Level-2 Ice Thickness data files are in ASCII text format (.mod) and contain fields for latitude, longitude, time, ice thickness, aircraft altitude, and confidence of thickness measurement.

Each .mod file is accompanied by an .xml metadata file. The metadata file contains information for date range, time range, geographic boundaries in latitude and longitude, platform, instrument, and campaign.

The PARIS radar data are separated into folders by date. Each folder contains the original files as they were output during the processing.

1.2 File Naming Convention

The ASCII text files are named according to the following convention and as described in Table 1.

```
20090401_PARIS_133608.par.mod
20090422PARIS_193607.par.mod
```

```
YYYYMMDD_PARIS_HHMMSS.par.mod
```

Where:

Table 1. File Naming Convention

Variable	Description
`YYYY`	four-digit year
`MM`	two-digit month
`DD`	two-digit day
`PARIS`	Pathfinder Advanced Radar Ice Sounder instrument
`HH`	two-digit hour
`MM`	two-digit minutes
`SS`	two-digit seconds
`.par`	indicates PARIS data file
`.mod`	indicates corrected ice thickness

1.3 File Size

The ASCII files range from approximately 12 KB to 332 KB.

1.4 Volume

Total volume of the data set is approximately 16 MB.

1.5 Spatial Coverage

The IceBridge PARIS campaign covers Greenland.

Southernmost Latitude: 60° N
Northernmost Latitude: 83° N
Westernmost Longitude: 73° W
Easternmost Longitude: 11° W

1.5.1 Spatial Resolution

The processed PARIS soundings have an along-track resolution of approximately 250 m and a depth resolution of 12.5 m.

1.5.2 Projection and Grid Description

These data are provided in unprojected geographic coordinates using the WGS84 vertical datum.

1.6 Temporal Coverage

The PARIS data were collected as part of Operation IceBridge funded campaigns and are available for ten days spanning 01 April 2009 to 02 May 2009.

1.6.1 Temporal Resolution

The data were collected in on April 1, 06, 17, 20, 22, 23, 24, 27, 28, and May 2, 2009. The processed delay Doppler data are in bins approximately 250 m along-track, making the instrument temporal resolution a variable function of aircraft velocity.

1.7 Parameter or Variable

The PARIS Level-2 Ice Thickness data set contains parameters for Ice Thickness in meters and Confidence of Thickness Measurement.

1.7.1 Parameter Description

The `*.par.mod` ASCII files contain fields as described in Table 2.

Table 2. File Parameters and Units

Column	Description	Units
`Latitude`	Latitude where data were collected.	Decimal Degrees
`Longitude`	Longitude where data were collected.	Decimal Degrees as negative East Longitude
`Time`	Time in seconds from midnight.	Seconds
`Ice Thickness`	Ice Thickness.	Meters
`Altitude`	Aircraft altitude. These values are not accurate; do not use them.	Meters
`Confidence of Thickness`	Confidence values range from 1 to 5. 1 - No thickness measurement due to verified geographic feature such as rocks, water, etc. 2 - No thickness measurement due to either geographic features, lack of instrument sensitivity, or signal clutter. 3 - Lowest confidence of detected bottom; bottom detected but either weak signal or multiple signal traces in echogram. 4 - Moderate confidence of detected bottom; stronger signal and no other possible bottoms in echogram. 5 - Highest confidence.	Integers 1 through 5

1.7.2 Sample Data Record

Below is an excerpt from data file `20090401_PARIS_133608.par.mod`. The columns have no headings. The six columns in each record correspond to the fields described in Table 2.

72.843740846	-30.363848398	73736.6481	48968.309248	2440.03467447	3
72.843000362	-30.3645171213	48968.923494	897.959106691	2437.24637141	3
72.8422590433	-30.36518861	48969.537743	885.306720585	2438.47637141	3
72.841519224	-30.365861244	48970.151992	878.980527532	2439.70437141	3

2 SOFTWARE AND TOOLS

The ASCII text files may be opened by any simple text reader.

3 DATA ACQUISITION AND PROCESSING

3.1 Theory of Measurements

The Delay-Doppler (DD) algorithm was developed at the Applied Physics Laboratory (APL) based on partially coherent processing of radar altimeter data. It has been shown that the DD technique can be applied very effectively to the ice-sounding problem. The first major benefit is that depth waveforms from a DD sounder have more degrees of freedom than any other technique. As is true for any radar, the received sounding signal is corrupted by speckle noise. This multiplicative noise is caused by the coherent combination of reflections from the many small individual scatterers within each range interval resolved by the system. Speckle noise can be reduced only by incoherent summation of statistically independent samples of the same reflectivity process. The DD algorithm maximizes incoherent integration, thus reducing the Signal-to-Speckle Ratio (SSR), which is a better SSR, while simultaneously balancing the improved spatial resolution due to coherent processing.

The second major benefit is that depth waveforms from a DD processor have much less interference from off-nadir returns. This means that where clutter includes all false competing signals appearing at the same depth the Signal-to-Clutter Ratio (SCR) is better than from incoherent integration and somewhat better than from coherent integration. The third benefit is that for non-specular scattering, the post-processing signal strength is better, that is, a better Signal to Noise Ratio (SNR), than from any other ice-sounding processing scheme, including coherent integration. These benefits are a direct consequence of the parallel integrations in multiple Doppler bins that enhance the desired waveform over both the multiplicative and the additive noise components. The practical result of these attributes is that the profiles have greater depth penetration and clutter rejection than are possible by any other means.

Fourth, and perhaps more subtle, the data are arrayed in range and Doppler space inside of the processor. For a given flight velocity V and radar wavelength lambda, there is a one-to-one relationship between Doppler frequency fD and the off-nadir angle theta in the plane of flight: fD = (2V/lambda)cos(theta). Thus, there is a one-to-one equivalence between the Doppler and the angular dimension; power arrayed in the range-Doppler domain is a mapping of the local scattering function. This domain within the DD ice-sounding algorithm provides an opportunity to select optimal depth and Doppler weighting to enhance the desired signals from depth.

Table 3 summarizes the first-order characteristics of potential radar sounder processing algorithms. The DD ice-sounder algorithm is a partially coherent integrator, using well-established techniques borrowed from synthetic aperture radar and advanced radar altimetry. The unique aspects of DD signal processing include block-by-block along-track Fast Fourier Transforms (FFTs) of the data into the Doppler frequency domain, followed by a phase multiplication or other means to correct the differential delay (off-nadir range-delay errors) of the along-track range measurement. The algorithm integrates over the history of reflections from each scatterer to form its range-delay measurement. This incoherent integration, performed in many parallel frequency-offset Doppler bins, is the basis for the advantages enjoyed by the delay/Doppler approach over both prior approaches.

Table 3. Signal Processing Strategies

Operation	**Incoherent**	**Coherent**	**Coherent (focused)**	**Delay-Doppler*** **
Pre-sum n pulses	Small n	Large n	Small n	Small n
FFT over m pulses=> m $f_D$bins*	n/a	n/a	n/a	Range-Doppler
Focusing kernal	n/a	n/a	Yes	(unfocused)
Migration (range delay correction)	n/a	n/a	Optional	Yes
Incoherent sums within each bin	n/a	n/a	n/a	Yes
Weight Doppler bins	n/a	n/a	Optional	Yes
Map scattering function**	n/a	n/a	n/a	Yes
Average (q waveforms)	Moderate q	Small q	Small q	Large q

* Doppler bin width (finesse) = PRF/m
** Backscattered power as a function of off-nadir angle
*** US Patent 6,188,341

Where:

n = number of pulses pre-summed.

q = number of pulses (waveforms) averaged.

m = number of pulses (after pre-summing) subjected to the FFT operation.

f_D bins = width (in Hz) of each Doppler bin.

Unfocussed indicates that in contrast to the coherent or SAR method, there is no focusing kernal needed for the delay-Doppler method. In other words, it is an unfocused SAR.
PRF/m = Pulse Repetition Frequency/m, that is, an FFT over m pulses at a given PRF divides the data into m bins of equal frequency width.

Optional indicates "users choice" the coherent method may or may not benefit from range delay correction, depending primarily on the interplay between resolution and the radar's altitude.

In practice, the number of parallel Doppler bins that can be usefully integrated depends on the encounter geometry. The dominant scattering mechanism is specular reflection for relatively flat layers illuminated by relatively long wavelength. In such cases the angular width of the backscattered signal is relatively small, typically less than a few degrees. This limit may impose an upper bound on the Doppler bins available for integration. Conversely, if the backscatter is from a non-specular rough surface, the resulting backscatter diagram is as wide as the illumination (Doppler) window. Thus, selective filtering in the Doppler domain can be exploited to reduce clutter.

Consider an example of processing optimization based on the range-Doppler data array. In the event that the surface return is specular and the return from depth is non-specular, as is the case over most of Greenland for example, then the Doppler bins filled by the surface return should be nulled out, and the higher-Doppler data used for penetration. This method will eliminate obscuration of the weak bottom signal by stronger sidelobes from the surface return.

Delay-Doppler data sets can be processed according to any or all of these ice-sounding algorithms. This will provide a robust and self-calibrated basis for quantitative comparison of the relative performance of these algorithms. An example of processed sounding data using incoherent, coherent, and DD algorithms is shown in Figure 1. DD is the only process that enjoys an improvement in spatial resolution and, simultaneously, a reduction in both clutter and speckle.

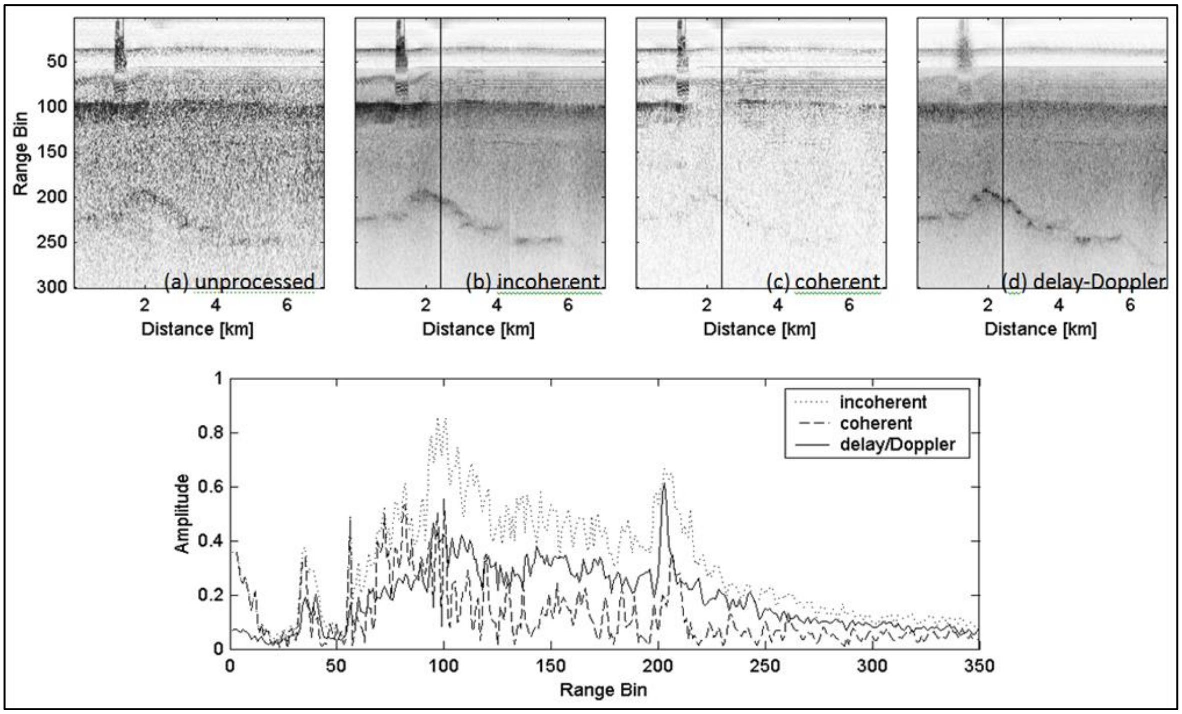

Figure 1. Processing Examples (a) Unprocessed data. (b) Incoherent-decreased speckle with no surface clutter or resolution improvement. (c) Coherent-decreased clutter and improved resolution but no speckle reduction. (d) DD-decrease in speckle and clutter, increase in SNR, and also with improved resolution. The plots on the bottom are amplitude traces corresponding to the vertical lines thought the images. Note: The respective differences between the processing methods increases with the altitude of the radar.

3.2 Data Acquisition Methods

The PARIS instrument was housed in two compartments within one standard 19-inch aircraft-qualified rack. The only additional components were computers used for programming, instrument control, and data acquisition. One compartment within the rack included the reference oscillator, the direct digital synthesis component, the ADCs, an FPGA, a USB interface, and a GPS receiver. All of these are commercial components. The FPGA was programmed through the USB interface prior to each use of the instrument. Once programmed, the FPGA accepted commands through the USB interface that configured system parameters such as pulse rate, pulse bandwidth, pulse length, step attenuator setting, variable attenuator setting, and sample rate. The FPGA also accepted commands to control the sounder operation to place it in standby mode, data collection mode including definition of the data collection interval, calibration modes, and test modes. The FPGA configured the DDS and triggered the generation of the transmit waveforms. The FPGA also accepted samples from the ADCs, buffered these, and transferred them to the USB interface. The USB interface provided an additional level of data buffering before the transfer of the data samples to the computers for recording.

All data samples, after possible presumming, were directly output to the computers over the USB interface, labeled removable storage in Figure 2. The USB interface to the laptop consisted of two software endpoints, one CONTROL IN/OUT endpoint for radar control and status, and one BULK IN endpoint for high-speed data transfer from the radar to the laptop. All data sent over the USB interface contained a checksum and were automatically re-transmitted upon error detection. The high-speed USB standard allowed transfer rates up to 60 MBytes/sec. The Integrated Circuit (IC) for PARIS has shown up to 32 MBytes/sec sustained transfer rates in practice, well within the sample rates required. The FPGA accepted a 1 PPS signal from the GPS receiver for sub-second time tagging of the sounder data. The GPS data were provided to the computers via an RS-232 serial interface and contained time and aircraft position data. The other compartment within the rack included the receiver and transmitter electronics. This included the filters, amplifiers, and switch on the transmitter side and the filters, amplifiers, switch, and attenuators on the receiver side.

The connections between the two compartments included a coaxial connector to carry the transmit waveform signal to the analog compartment, a coaxial connector to accept the received sounder data from the analog compartment, twisted-pair T/R switch and variable attenuator controller signals, and parallel signals to control the step attenuator. The additional connections were the two coaxial connections between the analog compartment and the antennas, and the front panel USB port (programming/command/data acquisition) and RS-232 (GPS time and position data) connections to the computer. Direct Current (DC) and Radio Frequency (RF) test ports were also included. Direct time segregation of the surface and bedrock returns prior to digitization was not possible in the long pulse design that would be required for an orbital sounder. The PARIS system was designed with sufficient dynamic range to adequately sample both returns simultaneously and time-segregate these returns in processing.

Digitization was performed with commercial devices with 12 or 14 bits at a 66.6 MHz rate. This is a higher rate than is required by the sounder, but it allowed for additional presuming if needed. The additional presumming allowed for the digitized data to be summed in hardware at pulse rates that are higher than those required for the DD processing in order to accumulate sufficient signal energy from the bottom of the ice sheet.

The only clock frequency present in the system was at 66.6 MHz and no multiples of this frequency were closer than 16.6 MHz to the 150 MHz RF frequency. Refer to Figure 5. The pulse bandwidth was only 5 MHz, so this frequency separation did not result in any contamination of the desired reflection signals by spurious power within the receiver. Furthermore, no local oscillator signals were present because no mixer stages were included in either the transmitter or the receiver. These were the factors that produced high linearity and minimized self-contamination of the sounding measurements.

The programming/control/data acquisition computer was a laptop computer connected to the sounder through the USB interface and to the GPS receiver through an RS-232 serial interface. In addition to the programming and data acquisition functions described above, this computer continually adjusted the transmit-receive interval during operational periods so that the collected data includes the range window of interest. The window normally included the top and bottom surfaces of the ice. Precision timing was not required, but the timing requirements were greater for the ice sounding demonstration than they were for the Doppler Phase-monopulse (D2P) altimeter demonstration because of the need to keep the surface return properly placed within the pass-band of the shaped filter. PARIS recorded all of the raw data for post-flight processing. While polarimetric analysis would, in theory, permit the reduction of side clutter in the data, it was not essential to include it for straightforward basement retrievals. So the basement depths given here were acquired by taking the returns to a single antenna and processing them as if they were from a PARIS-1 system.

3.3 Derivation Techniques and Algorithms

Analyzing the processed DD data for basement locations involved a multi-step algorithm. The first step was to identify the surface and basement locations at the beginning of the data set. To do this, the peaks of the first and second derivatives as well as of the original signal are used to help locate candidate surface/bottom locations. After the initial seed locations are found, the candidate locations in the adjacent return signals are weighted based on the magnitude of the distance from the last detected surface/bottom locations and the calculated amplitudes of the signals at those locations. The peaks of the derivatives are used again to help identify the top/bottom positions within the signal. These successive surface/basement pairs utilize a window that limits the allowable distance of the detected surface/basement locations from the previous ones. Each individual data file was then plotted and manually reviewed. This review consists of:

- Identification of areas where the surface/basement following algorithm failed
- Rectification of the erroneous detections
- Assignment of a 'confidence level' to each data point

The data were plotted along with the detected surface/basement locations and an estimate of the possible locations of aircraft reflections which the algorithm could confuse with a surface or basement location. By means of the graphic user interface, the analyst can then either suggest the area in which to automatically re-search for the correct surface or bottom, or explicitly mark where it should be in cases where the algorithm fails completely.

In addition, each data point was manually assigned a confidence level, which indicates to the end user the confidence in the algorithm and the analyst's manual interventions. Once the manual inspection of a data file is complete, the results are saved to an ASCII file in both uncorrected and corrected format. The corrected format divides the distance between the surface and basement by a factor of 1.78, whereas the uncorrected format does not.

3.3.1 Processing Steps

The PARIS data processing has historically used a coefficient of 1.78 to convert calculated distance through air into distance through ice. After the processing software determines the distance between the surface reflection and bottom reflection in air, it divides that value by 1.78 to convert to distance through ice.

The following processing steps are performed by the data provider:

1. Load data file into processing software to automatically identify local maxima of the return waveform and determine bedrock elevation using both return signal strength and elevation of previous bottom measurement.
2. Scroll through the echograms, highlighted with identified bedrock elevation from the previous step, and correct bed elevation where the algorithm incorrectly selected the bottom.
3. Scroll back through echogram and modify the confidence of each bottom measurement, where necessary, based on the confidence definitions.

Definitions of Confidence Levels:

- Level 1 - No thickness measurement due to verified geographic feature such as rocks, water, etc. It is expected that no bed rock elevation measurement would be possible for this location.
- Level 2 - No thickness measurement due to either geographic features, lack of instrument sensitivity, or signal clutter. It is expected that a bed elevation measurement should be possible for this location, but no measurement was recovered.
- Level 3 - Lowest confidence of detected bottom: bottom detected but either weak signal or multiple signal traces in echogram. The most reasonable maximum in the return waveform was selected as the bedrock location, but it is possible that one of the other maxima could be the actual bedrock location.
- Level 4 - Moderate confidence of detected bottom: stronger signal and no other possible bottoms in echogram.
- Level 5 - Highest confidence. Due to return signal strength and lack of other maxima in the waveform, there is a very high likelihood that the indicated bedrock location is correct.

3.3.2 Error Sources

For 2009 Greenland data, do not use any measurements labeled with a confidence value of 1 or 2. There will be thickness values for these measurements, but these values are known to be incorrect.

Do not use the Altitude measurements for 2009 Greenland. The values are not correct.

3.4 Sensor or Instrument Description

The PARIS radar sounder demonstrates a new and simpler architecture permitted by recent advances in digital electronics. The primary motivation for the innovations was to assure linearity sufficient to support the requirements imposed by ice sheet sounding from a remote platform to depths of several kilometers. The radar data are brought into the digital domain after a minimum number of analog processing steps. This improves the linearity of the entire system, which among other benefits substantially reduces the spurious inter-modulation products that could otherwise contaminate the data. Figure 2 shows the block diagram of the PARIS system deployed for IceBridge.

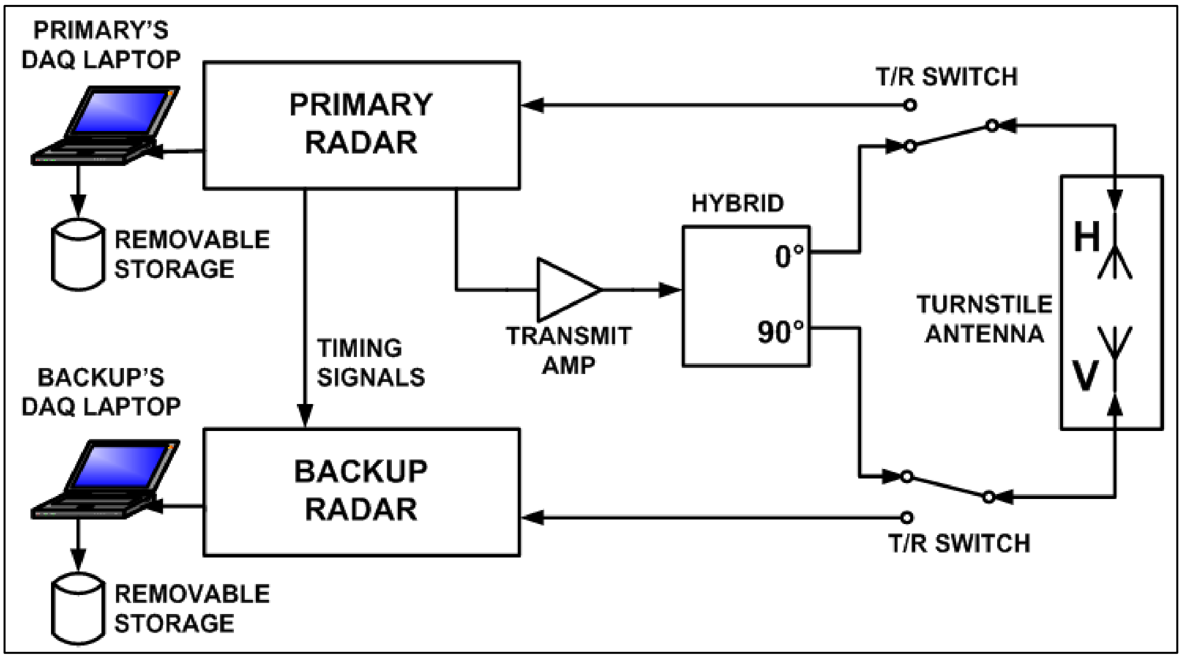

Figure 2. PARIS Block Diagram

The operational specifications of the PARIS radar are shown in Table 4.

Table 4. Operational Specifications of PARIS Radar

Radar Type	Chirped-pulse
Center frequency	150 MHz
Bandwidth	6 MHz
Peak power	250 W
Range resolution	17 m in ice
Pulse rate	8-10 kHz
Pulse width	3-30 μs
Input noise figure	4 dB

Radar Type	Chirped-pulse
Antenna	Turnstyle
Antenna polarization	Coupled H and V
Antenna gain	10 dBi
Prime power requirement	500W
Electronics mass	110 kg
Electronics volume	350 dm3 estimated

3.4.1 Transmit Path

The transmit waveform is a 5 MHz bandwidth chirp generated by a commercial Direct-Digital Synthesizer (DDS) chip. The chip also applies a trapezoidal envelope to the pulse, minimizing unwanted sidebands. The 250 W amplifier uses a class AB mode of operation to ensure high linearity and thus preserve the pulse's low sidebands. Bench tests of the amplifier demonstrated a two-tone third-order inter-modulation of better than -20 dBc measured at P_O = 250 W.

Since polarimetric mode operation required two receive channels, the task might have been costly in time and money to achieve if a two-channel radar had been built from scratch. However, given that two copies of the PARIS-1 radar used in 2007 were fabricated for the original task as primary and backup respectively, it was decided instead to use them both, operating in tandem as shown in Figure 2.

The antennas used in the original 2007 mission were designed for only one linear polarization, so for polarimetric operation it was necessary for the APL to design a new antenna for the P-3 aircraft for use by the modified PARIS-2 arrangement during the IceBridge missions. Figure 3 shows the new turnstyle antenna as mounted in the bomb bay of the P-3, both externally and internally within its fiberglass radome. The styrofoam members added to the interior of the radome are for support of the turnstyle antenna, and are transparent to 150 MHz transmissions. Time constraints prevented the full characterization of this new antenna prior to the Ice Bridge flights.

Figure 3. Placement of PARIS Radar Antennas on the NASA P-3 Aircraft

Another significant change from the original PARIS operation mode was the necessity to deal with antenna sharing between transmitter and receiver. This came about as a consequence of insufficient room on the NASA P-3 to mount separate transmit and receive antennas, as were used during the 2007 PARIS flights. Fast, high-power Transmit/Receive (T/R) switches, as indicated in Figure 2, were required to switch the antennas between their respective transmit and receive path.

Another consequence of this change was a reduction in receiver sensitivity, the mitigation of which was prevented by the urgency of the schedule. However, since the radar was secondary to NASA's Airborne Topographic Mapper (ATM), and since use of the ATM required the aircraft to fly relatively close to the ice, it was felt that the consequent reduction in path loss would likely compensate for the loss of sensitivity. This turned out be true in much of the collected data.

3.4.2 Receive Path

Since the radar sampled the Radio Frequency (RF) signal directly, there was no down-conversion or Intermediate Frequency (IF) signal within the receiver. This greatly reduced the complexity of the analog section of the receiver. Immediately following the receive antenna was an absorptive transmit-receive switch to provide two levels of protection for the Low Noise Amplifier (LNA) during the transmit cycles. The signal continued through amplification and filtering stages, without being down-converted. Variable-gain amplifiers were employed to permit sensitivity time control, which increased the overall dynamic range of the system. Refer to Figure 4. Total gain of the receive chain was 65 to 95 dB, with a +45 dBm third-order input intercept point. Bandpass filters ensured that the subsequent undersampling operation was uncontaminated.

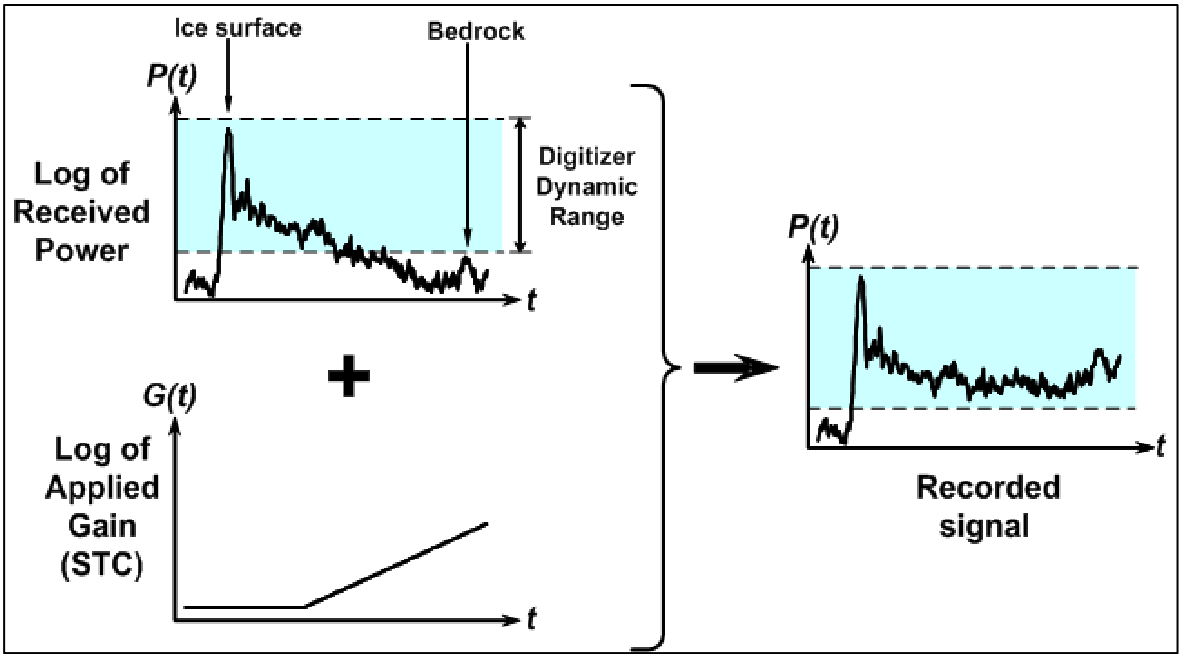

Figure 4. Effect of Sensitivity Time Control (STC)

3.4.3 Digital Section

The digital section of the radar contributed most of the functionality within, and permitted miniaturization not formerly seen in ice sounders. During pulse transmission, the Field-Programmable Gate Array (FPGA) configured and triggered the DDS to directly generate a transmit pulse at the 150 MHz operating frequency, which was then amplified by the power amplifier and emitted by the antenna. During reception, the FPGA accepted the undersampled data stream from the Analog-to-Digital Converter (ADC), filtered it digitally and buffered it for transfer to the data acquisition laptop via a USB 2.0 interface. Figure 5 shows the frequency plan of the undersampling strategy used.

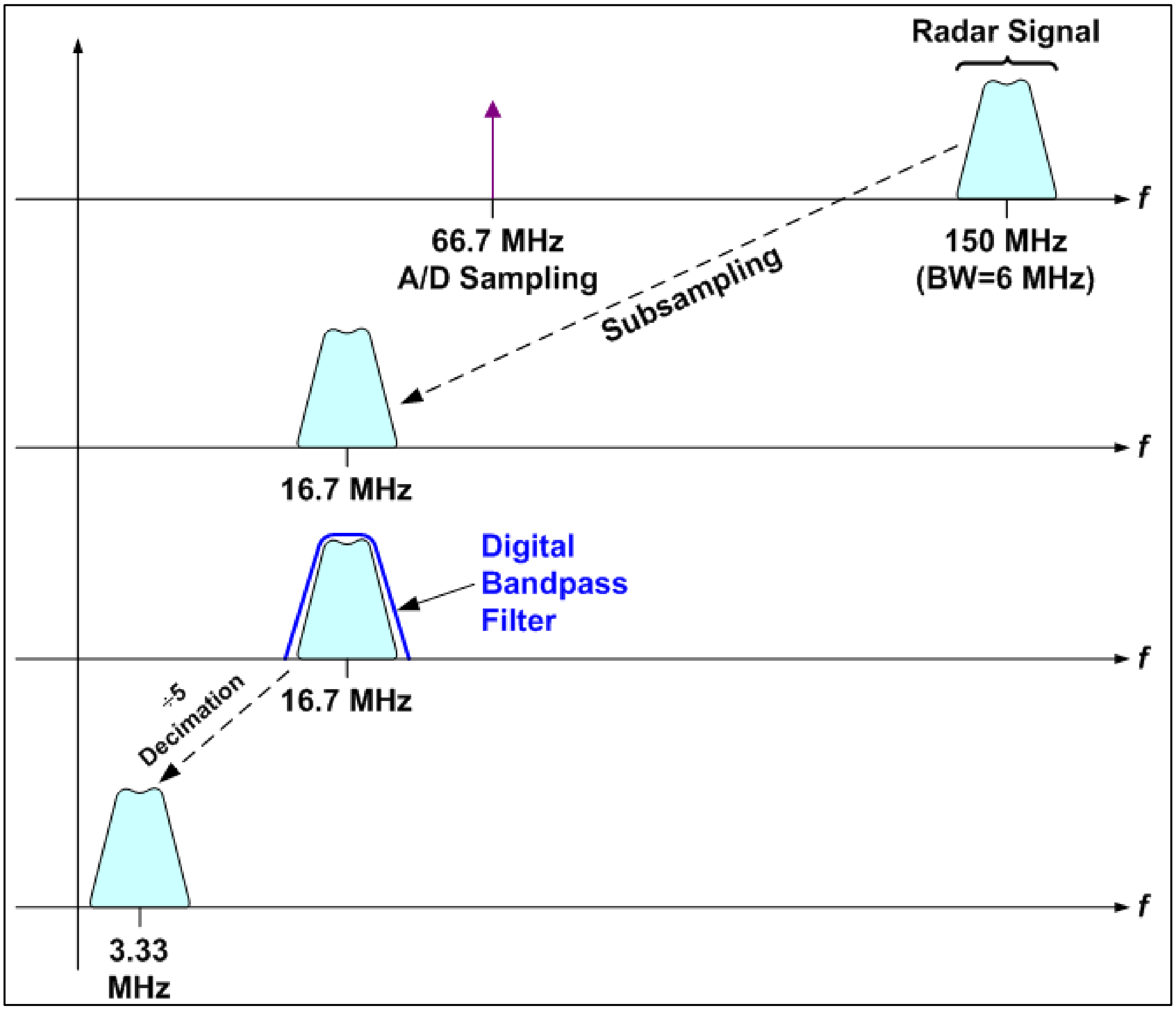

Figure 5. PARIS Radar Undersampling Frequency Plan

Figure 6 shows examples of the digital processing performed by the FPGA.

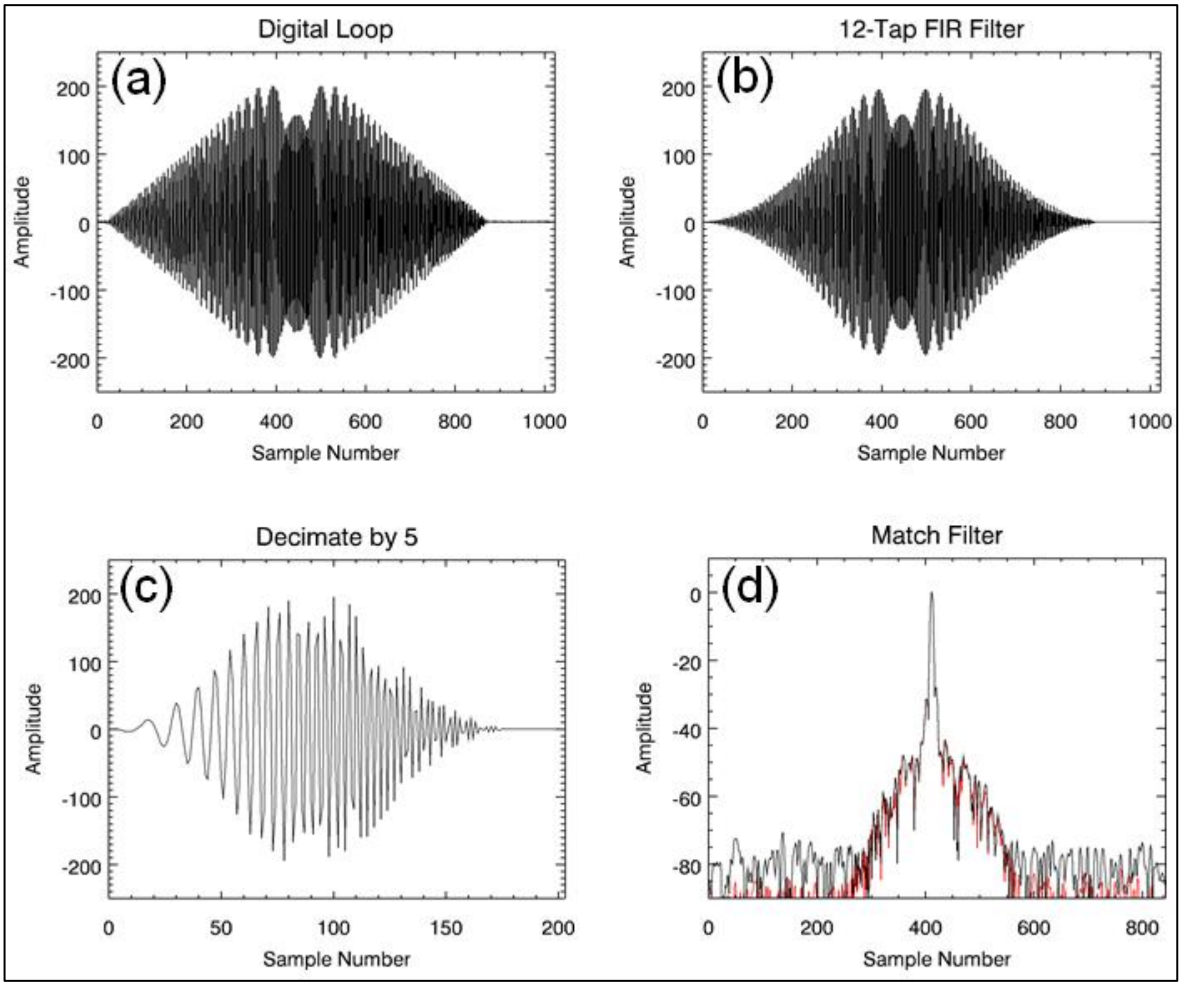

Figure 6. Waveform Representation of the Data Processing. (a) Shows a transmit waveform centered on 16.67 MHz after being undersampled at 66.7 MHz. (b) Shows the same waveform after being passed through the Finite-Impulse Response (FIR) digital bandpass filter. After decimation-by-5, the waveform appeared as in (c), sampled at 13.33 MHz, and centered on 3.33 MHz. If a matched filter is applied to this waveform by cross-correlating it with an analytical replica of the transmit waveform, the result can be seen in (d), demonstrating sidelobe levels of -40 dB below peak.

The FPGA time-tags each transmit pulse by relying on a one pulse-per-second (PPS) signal from a GPS receiver. The time tag is used during processing to geolocate each radar pulse. The FPGA also paces radar transmission pulses and supervises application of STC gain changes. All components of the digital subsection are clocked by a stable 400 MHz reference oscillator.

4 REFERENCES AND RELATED PUBLICATIONS

4.1 Related Data Collections

IceBridge MCoRDS L2 Picked Ice and Bed Surfaces and Ice Thickness

Greenland 5 km DEM, Ice Thickness, and Bedrock Elevation Grids

IceBridge HiCARS 1 L2 Geolocated Ice Thickness

4.2 Related Websites

IceBridge Data Web site at NSIDC

IceBridge Web site at NASA

ICESat/GLAS Web site at NASA Wallops Flight Facility

ICESat/GLAS Web site at NSIDC

5 CONTACTS AND ACKNOWLEDGEMENTS

Matthew Linkswiler
NASA Goddard Space Flight Center
Wallops Flight Facility
Wallops Island, Virginia 23337-5099

Keith Raney
Applied Physics Laboratory (APL)
John Hopkins University
Laurel, Maryland 20723

Acknowledgments:

The instrument development and field campaign were funded under grants from NASA.

6 DOCUMENT INFORMATION

6.1 Publication Date

06 October 2011

6.2 Date Last Updated

04 October 2012